



# Single Particle Orbits in a Tandem Mirror

L.L. Lao, R.W. Conn, and J. Kesner

May 1978

UWFDM-245

***FUSION TECHNOLOGY INSTITUTE***

***UNIVERSITY OF WISCONSIN***

***MADISON WISCONSIN***

# **Single Particle Orbits in a Tandem Mirror**

L.L. Lao, R.W. Conn, and J. Kesner

Fusion Technology Institute  
University of Wisconsin  
1500 Engineering Drive  
Madison, WI 53706

<http://fti.neep.wisc.edu>

May 1978

UWFDM-245

"Single Particle Orbits in a Tandem Mirror"

L. L. Lao  
R. W. Conn  
J. Kesner

UWFD-245

Fusion Research Program  
Nuclear Engineering Department  
University of Wisconsin  
Madison, Wisconsin 53706

To be published in Nuclear Fusion.

## I. Introduction

In a tandem mirror,<sup>(1,2)</sup> two minimum-B magnetic wells are connected by a uniform solenoid. The magnetic flux tubes in the minimum-B plugs entering the solenoid can be oriented to face one another (i.e., be parallel) or they can be orthogonal. The two cases are illustrated in Fig. 1. The parallel case has sometimes been considered in the design of tandem mirror experiments. However, from single particle orbit calculations, we find that a class of particles will appear in the parallel joining case which generate elliptical drift surfaces that can be detrimental to central cell particle confinement. In either case, the joining of elliptical flux tubes in the plugs to the central solenoid introduces regions of sufficiently bad curvature that the plug ions which penetrate deeply into the magnetic well begin drifting unfavorably in the azimuthal direction. In this note, we summarize findings on the single particle orbits in the University of Wisconsin RF heated tandem mirror experiment, PHAEDRUS.<sup>(3)</sup> Although calculations are performed using this particular magnetic field configuration, the results are general and can be applied to other tandem mirror experiments.

## II. Equations of Motion

The guiding center motion of a particle in a tandem mirror is to first order a superposition of the parallel motion along magnetic field lines and a perpendicular drift induced by the curvature and the non-uniformity

of the field lines. This motion is described in the non-relativistic case by the following pair of equations:

$$\frac{dv_{\parallel}}{dt} = -\frac{\mu \bar{\nabla} B}{m} \cdot \frac{\bar{B}}{B} + \frac{q}{m} \frac{\bar{E} \cdot \bar{B}}{B} \quad (1)$$

$$\bar{v}_{\perp} = \frac{\bar{E} \times \bar{B}}{B^2} - \frac{\mu \bar{\nabla} B \times \bar{B}}{qB^2} + \frac{mv_{\parallel}^2}{q} \frac{\bar{B}}{B^2} \times \left( \frac{\bar{B}}{B} \cdot \bar{\nabla} \right) \frac{\bar{B}}{B} \quad (2)$$

Essential to this guiding center approximation is the constancy of the magnetic moment,  $\mu = \frac{1/2mv_{\perp}^2}{B}$ . This is valid as long as the confining magnetic field does not vary rapidly in space or over a gyration period. Equations (1) and (2) are solved numerically for the particle guiding center orbit using a computer code obtained from the Lawrence Livermore Laboratory (LLL).<sup>(4)</sup> The magnetic fields are calculated given the position of the current carrying elements. For the plug ions, the electric field terms are left out. For the central cell ions, the electric fields are assumed to be zero in the solenoid and have a constant value around the central region of the plugs.

### III. Results

#### 1. Magnetic Field Configuration

We summarize here the main characteristics of the magnetic field<sup>(5)</sup> used in the calculations. The plugs are Ioffe-coil-stabilized mirrors while the central cell consists of circular coils and two recircularizing coil sets. The latter coils connect the central cell to the two minimum-B end plugs. The origin of the coordinate system is at the center of the solenoid and the Z-axis is along the mirror longitudinal axis. The Ioffe

bars are located at  $\theta = 0^\circ, 90^\circ, 180^\circ$  and  $270^\circ$ . This is shown in Fig. 2(a). In Fig. 2(b), we show the variation of  $|\bar{B}|$  in the  $z$  direction. The field is fairly uniform at 400 G in the solenoidal central portion up to the recircularizing region. In that zone, the magnetic field rises rapidly to 3200 G at the mirror throat. It then decreases to 1750 G at the plug mid-plane. With this particular coil arrangement, the elliptical flux tubes in the plugs are oriented facing each other. The last closed flux surface is a circle of radius 8 cm at the plug mid-plane and 17 cm at the central cell mid-plane.

The orthogonal joining case can be obtained by rotating all the conductors to the right of the central cell mid-plane  $90^\circ$  azimuthally. In Fig. 3, we show plots of two field lines in the planes  $\theta = 45^\circ$  and  $\theta = 135^\circ$  that map the circle of radius 8 cm at the plug mid-plane into the central cell mid-plane.

## 2. Particle Drift Surfaces

Calculations have been done for both  $H^+$  and  $D^+$  ions with energies of 1 keV in the plugs and approximately 10 eV in the central cell. This is typical of parameters expected in the PHAEDRUS experiment. In Figs. 4 to 5 we show plots of particle drift surfaces in the plane  $z = \text{constant} = \text{ZCROSS}$  for various sets of ion initial parameters: the perpendicular energy  $W_\perp$ , parallel energy  $W_\parallel$ , and initial position  $\bar{r}_0$ . The points plotted are those where the ion crosses this  $z = \text{ZCROSS}$  plane; plus (+) marks indicate the ion is moving in the positive  $z$  direction while minus (-) marks indicate the ion is moving in the negative  $z$  direction. The arrow shows the net ion rotating direction. These ion drift surfaces can be roughly classified as follows:

### A. Central Cell Ions

#### a. Magnetically trapped ions with large initial $\frac{W_{\perp}}{W_{\parallel}}$

These ions remain near the central portion of the solenoid where the field is fairly uniform. They show unfavorable azimuthal drift and generate circular drift surfaces. A typical case is shown in Fig. 4(a) for an ion started **initially in the solenoid mid-plane** at  $r = 6$  cm.

#### b. Magnetically trapped ions with small initial $\frac{W_{\perp}}{W_{\parallel}}$

These ions penetrate deeply into the magnetic well and spend considerable time in the recircularizing sections. Since  $\bar{v}_d \sim -\frac{\mu \bar{\nabla} B \times \bar{B}}{B^2}$ , the azimuthal component  $B_{\theta}$  from the recircularizing Ioffe bars crossed with  $(\bar{\nabla} B)_z$  causes the ion to drift radially. We can distinguish two cases:

##### (i) The elliptical flux tubes in the plugs are oriented facing each other

In this case both  $B_{\theta}$  and  $(\bar{\nabla} B)_z$  have opposite signs on either side of the central cell mid-plane. Thus, the radial drifts reinforce each other as the ions travel successively from one side of the cell to the other causing a net outward radial drift in the quadrant  $\theta_1 = -45^{\circ}$  to  $\theta_2 = -135^{\circ}$  as they drift slowly and unfavorably in the clockwise azimuthal direction. As the ions pass to the next quadrant with  $\theta_1 = -135^{\circ}$  to  $\theta_2 = -225^{\circ}$ , they drift radially inward since  $B_{\theta}$  changes sign. Thus, the ion drift surfaces are elliptical. A typical case is shown in Fig. 4(b) where the ion motion begins at the solenoid mid-plane. Depending on the orientation of the initial ion velocity vector with the magnetic field, the elongation of one axis of these ellipses relative to the other varies from one to two.

(ii) The elliptical flux tubes in the plugs are orthogonal to each other

For this case, the ions' radial drifts tend to cancel each other as they pass successively through the cell mid-plane because  $B_\theta$  now has the same sign in the two recircularizing sections while  $(\bar{\nabla}B)_z$  changes sign. The ions drift mainly in the unfavorable azimuthal direction and their drift surfaces are circular. In Fig. 4(b), we show a typical case where the ion motion begins at the mid-plane.

c. Electrostatically Confined Ions

These ions have large initial  $\frac{W_{\perp}}{W_{\parallel}}$  allowing them to pass through the mirrors and travel to the central region of the end plugs. The electrostatic field then causes the ions to turn around. This effect is modeled in the code by a constant electric field in the z direction around the central region of the plugs. Depending on the relative orientation of the two plug flux tubes, the drift surfaces are either elliptical or circular. These are shown in Fig. 4(c).

B. Plug Ions

a. Ions with large initial  $\frac{W_{\perp}}{W_{\parallel}}$

These ions are trapped near the plug central region which has both good curvature and small  $(\bar{\nabla}B)_z$ . Thus, they have favorable azimuthal drift but negligible radial drift. Their drift surfaces are circular. In Fig. 5(a), we show a typical case for an ion that begins its motion at the mid-plane.



b. Ions with small initial  $\frac{W_{\perp}}{W_{\parallel}}$

These ions penetrate deeply into the magnetic well and spend considerable time in the bad curvature region present near the mirror throat. They therefore have a net unfavorable azimuthal drift. Furthermore,  $(\vec{\nabla}B)_z$  is large and has the opposite sign near the mirror throats.  $B_{\theta}$  retains the same sign so that the radial drifts are noticeable and opposite on the two sides of the plug mid-plane. Ions in this class oscillate radially as they drift unfavorably in the azimuthal direction. The drift surface they generate at the plug mid-plane consists of two ellipses rotated  $90^\circ$  with respect to each other. A typical case is shown in Fig. 5(b). The ion motion begins in the plug mid-plane at  $r = 6.5$  cm.

#### IV. Discussion

##### 1. Central Cell Ion Orbits

In general, the ions confined in the central cell region of a tandem mirror have good orbits and a very slow but unfavorable azimuthal drift. However, if the flux tubes of the two end plugs are joined facing each other (in parallel), ions penetrating deeply into the magnetic well as well as those confined electrostatically will drift radially. Thus, there is a critical radius for an ion with given initial  $\mu$  and  $W$ . An ion beginning its motion outside this radius will drift radially and will be lost either because it hits the chamber wall or because it does not see the electrostatic potential in the plugs. We plot in Fig. 6 the fraction of electrostatically confined ions lost due to this elliptical drift surface,  $F(r)$ , versus the ion initial radius in the mid-plane. The result is based on averaging over the ion initial azimuthal angle as well as over the time which the ion spends at different radii of the

elliptical drift surface. The total fraction of electrostatically confined ions lost due to the elliptical drift surface is obtained by integrating  $F(r)$  over the ion radial density profile. This is given in Table 1 for various ion density radial dependences. If the end plug flux tubes are orthogonal to one another, the radial drifts tend to cancel and the ions have circular drift surfaces. Clearly this is the preferable situation so that end plugs in tandem mirrors should have flux tubes joined orthogonally. In either case, all ions drift unfavorably in the azimuthal direction. This is particularly true for those ions that penetrate deeply into the magnetic well or that are confined electrostatically. These unfavorable drifts may cause microinstability.

## 2. Plug Ion Orbits

Similar to the central cell ions, the plug ions trapped in the central region have good orbits and they drift favorably in the azimuthal direction. Those ions penetrating deeply into the magnetic well have unfavorable azimuthal and radial drift. For the magnetic field configuration of PHAEDRUS, this critical angle is  $60^\circ$  measured from the z-axis. (If the initial ion velocity vector makes an angle less than or equal to  $60^\circ$  with the z-axis, it will drift unfavorably). The loss cone is about  $49^\circ$ . Thus, we estimate the fraction of ions drifting in the unfavorable direction to be roughly 5% or less. This can be reduced by modifying the relative currents in the mirror and Ioffe coils if greater radial well depth is required.

## V. Conclusion

We find that flux tubes from the minimum-B end plug in a tandem mirror must be joined orthogonally to prevent a deterioration of particle

containment in the central cell due to the appearance of elliptical drift surfaces. For all cases, all central cell ions and sometimes a small fraction of plug ions have unfavorable azimuthal drift.

#### Acknowledgement

We would like to thank Dr. R. Post for many useful discussions. We are also grateful to Dr. J. Foote and Dr. S. Devoto at Lawrence Livermore Laboratory for making the single particle orbit code available to us. This research was supported by U.S.D.O.E.

#### References

1. G. I. Dimov, V. V. Zakaidakov, and M. E. Kishinevsky, "Open Trap with Ambipolar Mirrors", in Plasma Physics and Controlled Nuclear Fusion Research (Proc. 6th Int. Conf. Berchtesgaden, 1976) 3, IAEA, Vienna (1977) 177.
2. T. K. Fowler and B. G. Logan, "The Tandem Mirror Reactor," Comments on Plasma Physics and Controlled Fusion Research, Volume II, No. 6, 167 (1977).
3. R. S. Post, J. Kesner, J. Scharer, R. Conn, "An RF Heated Tandem Mirror Experiment," Bull. Am. Phys. Soc. 22, 1094 (1977).
4. W. A. Perkins, D. Fuss, "MAFCO II", Lawrence Livermore Laboratory Report UCRL-50438 (1968).
5. J. Kesner, L. P. Mai, R. S. Post, "Design Characteristics of the Wisconsin RF Heated Tandem Mirror", Bull. Am. Phys. Soc. 22, 1094 (1977).

Table 1

Total fraction of electrostatically confined ions lost due to the elliptical drift surfaces as a function of the radial density profile in the central cell.

$$n(r) = n_0 \left( 1 - \left( \frac{r}{r_{\max}} \right)^{2\alpha} \right)$$

$\alpha$	0.0	0.5	1.0
Total Fraction Lost	0.16	0.12	0.09

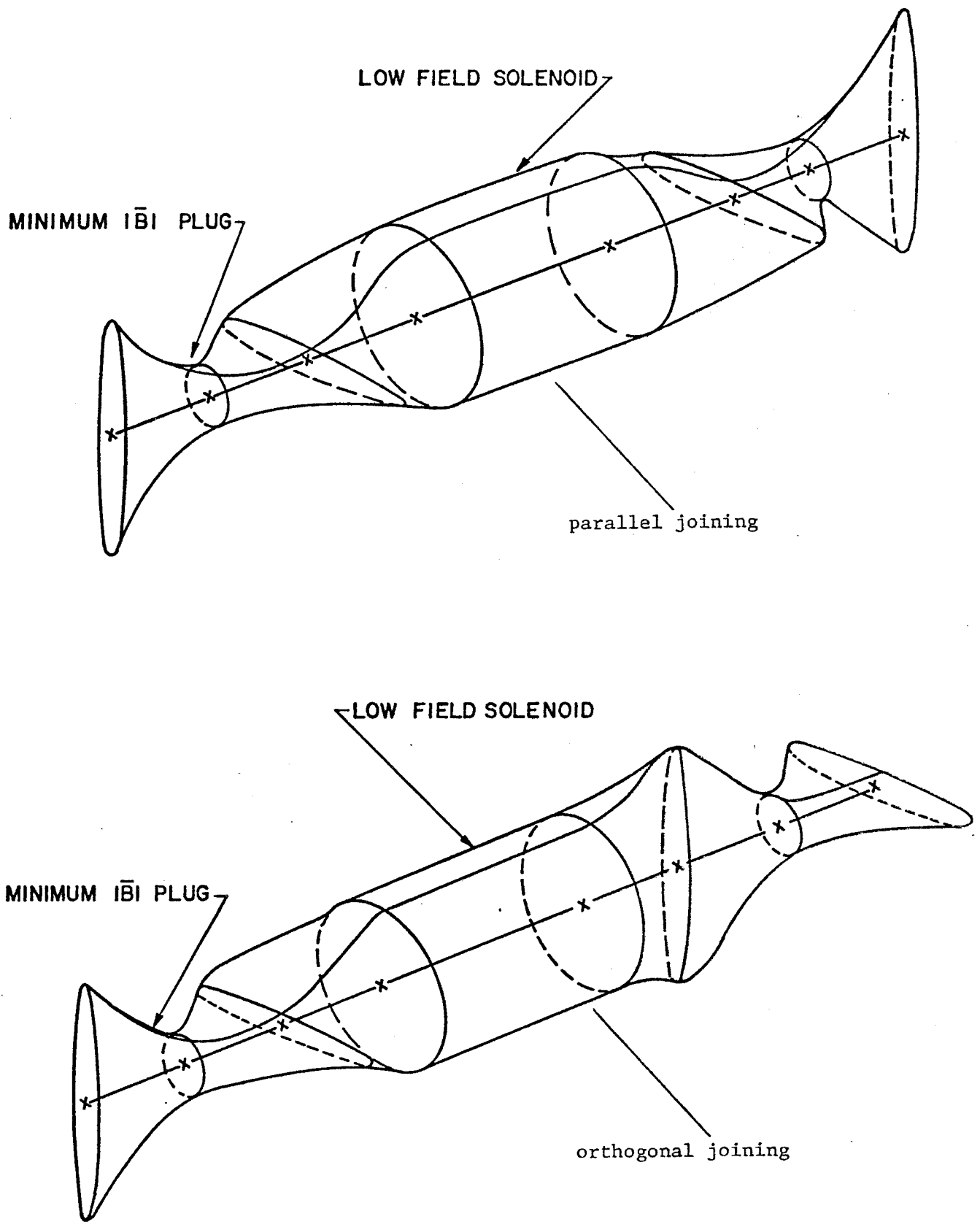


Fig. 1

CIRCULARIZED TANDAM MIRROR EFF1 CALC 10 03:29:54A 10/19/77  
 FIELD MAGNITUDE ALONG FLUX LINES 1 THROUGH 2

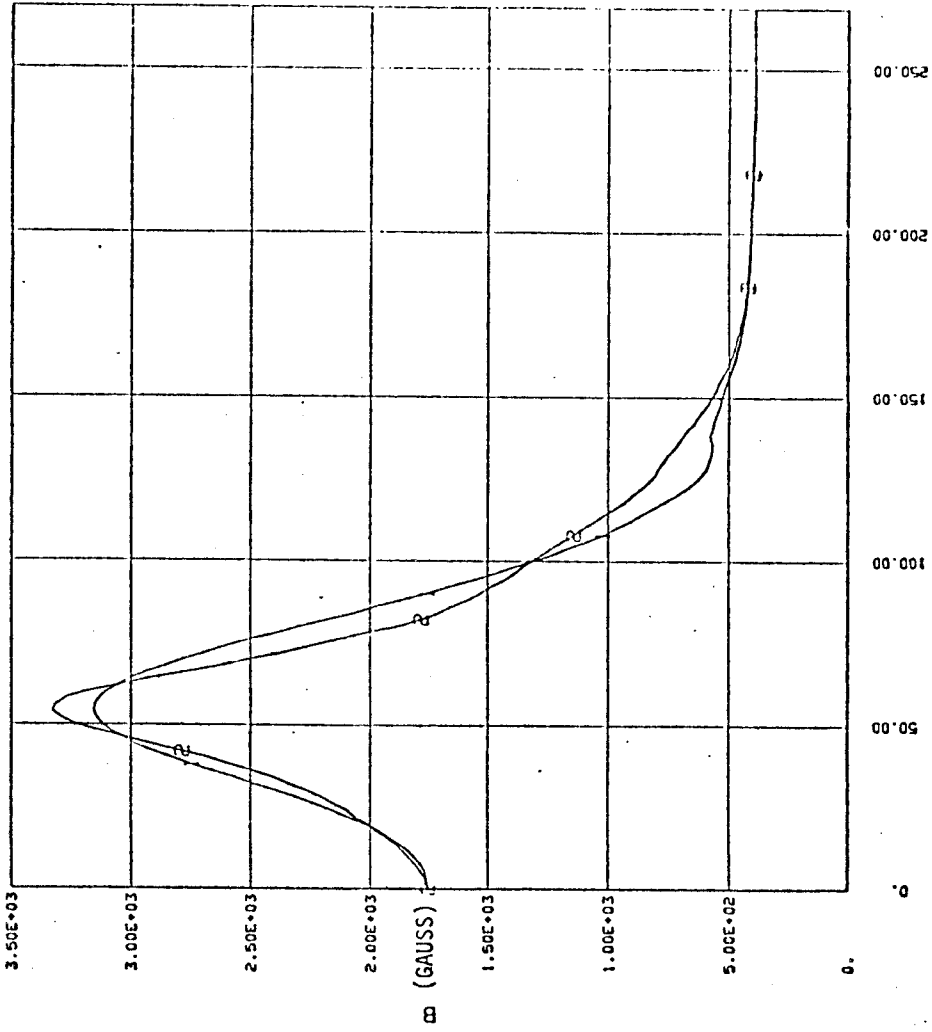


Fig. 2b  
 Plot of  $|\vec{B}|$  along a field line

RES. TANDAM MIRROR COILS  
 DATA 1 120.0 EFF1 = 123.0 NU = 30.0

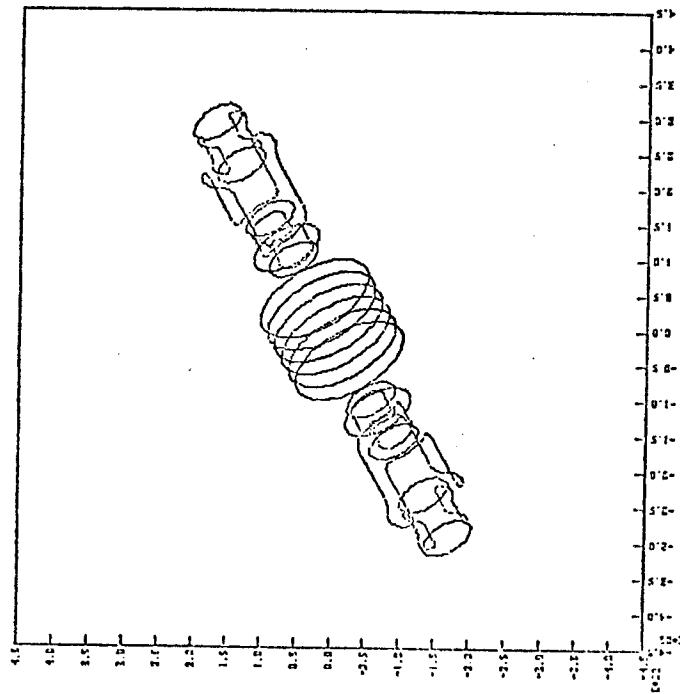


Fig. 2a

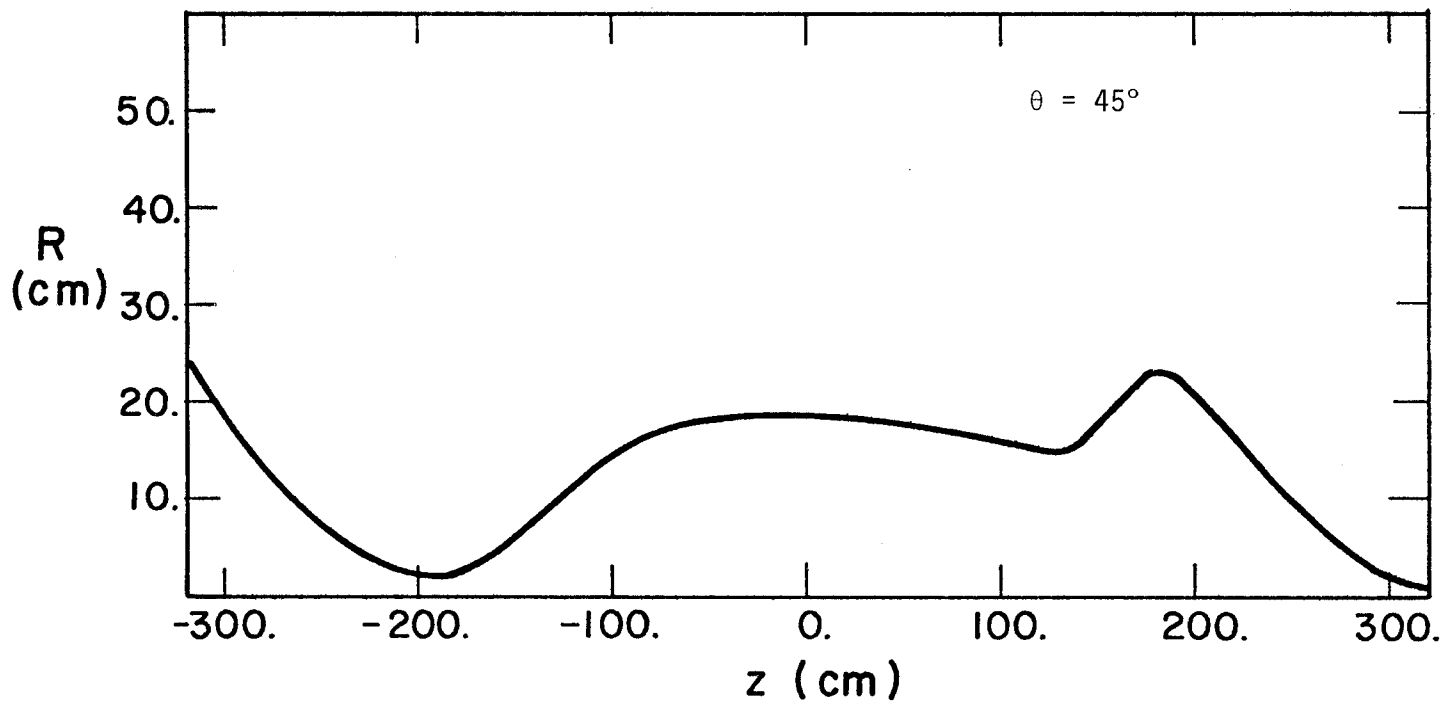
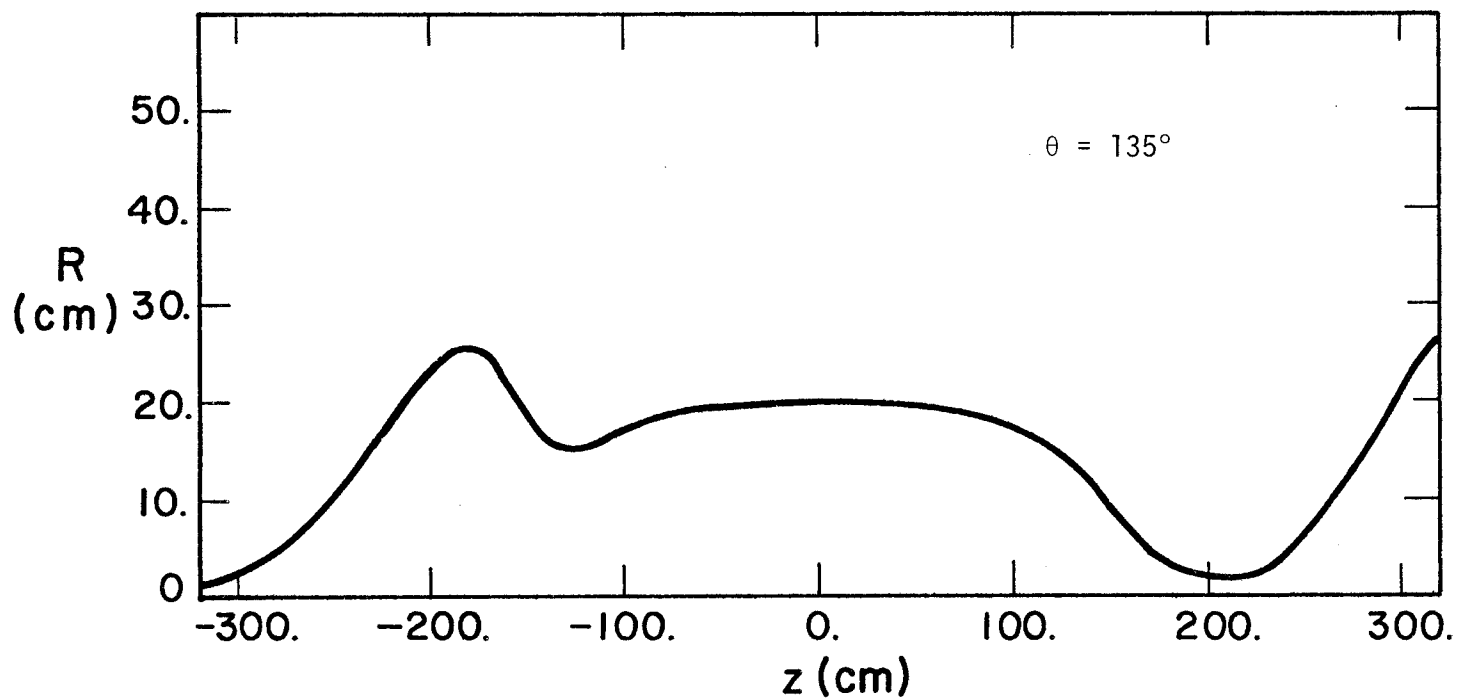
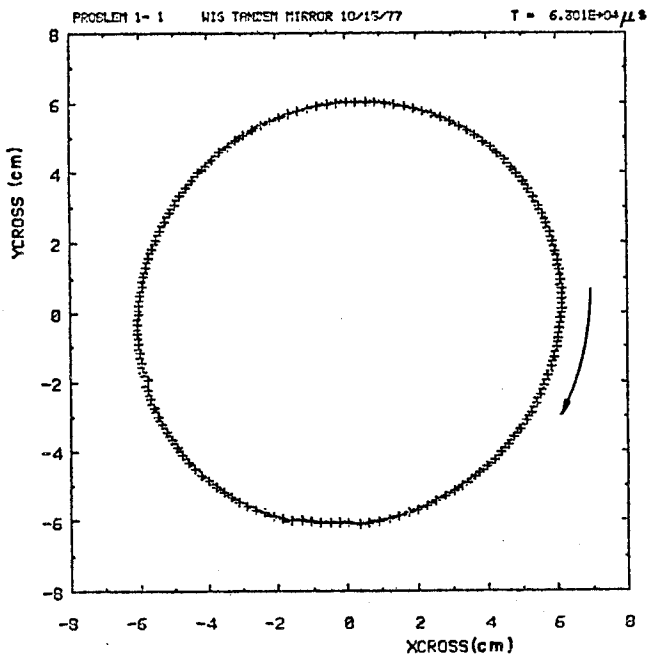
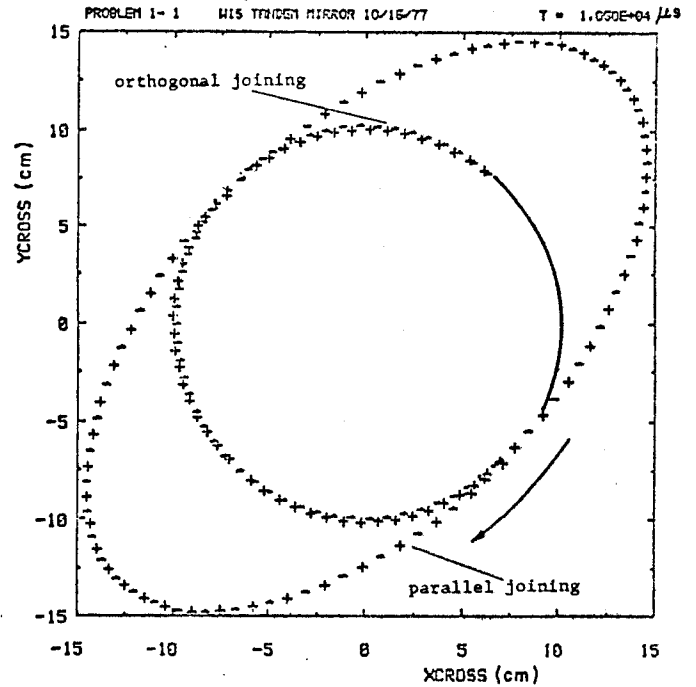


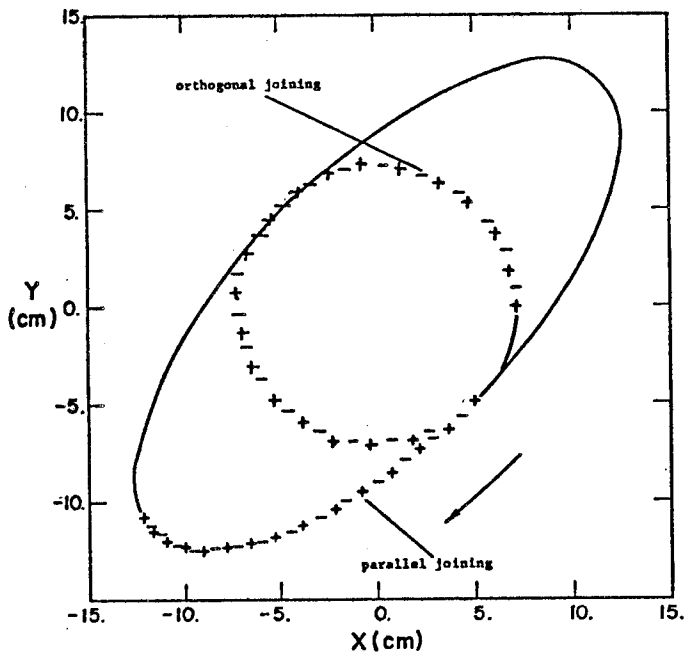
Fig. 3. Plots of field lines in the planes  $\theta = 45^\circ$  and  $\theta = 135^\circ$ . The flux tubes in the plugs are joined orthogonally.



(a)



(b)



(c)

Fig. 4. Central cell ion drift surfaces in the central cell mid-plane  $z_{\text{cross}} = 0$ .  
 (a) Magnetically confined  $D^+$  ion,  $W_{\perp}(0) = 9$  eV,  $W_{\parallel}(0) = 1$  eV,  $r(0) = 6$  cm.  
 (b) Magnetically confined  $H^+$  ion,  $W_{\perp}(0) = 2$  eV,  $W_{\parallel}(0) = 10$  eV,  $r(0) = 10$  cm,  
 $\theta(0) = -45^\circ$ . (c) Electrostatically confined  $H^+$  ion,  $W_{\perp}(0) = .5$  eV,  
 $W_{\parallel}(0) = 11.5$  eV,  $r(0) = 7$  cm,  $\theta(0) = -45^\circ$ . Ioffe bars are at  $\theta = 0^\circ$ ,  
 $90^\circ$ ,  $180^\circ$  and  $270^\circ$ .



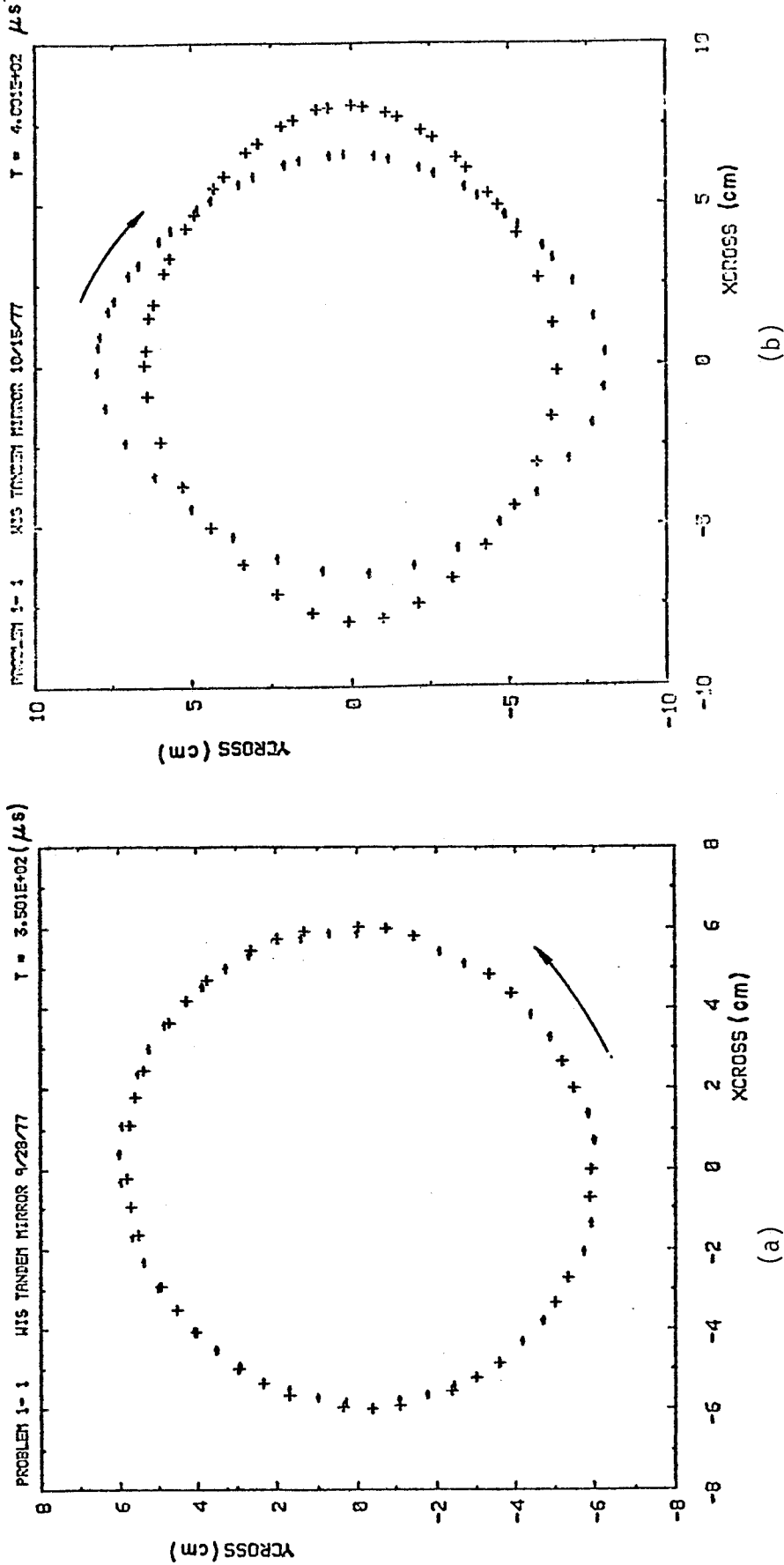


Fig. 5. Plug ion drift surfaces in the plug mid-plane ZCROSS = 260 cm. (a)  $D^+$  ion,  $W_{\perp}(0) = 1$  KeV,  $W_{\parallel}(0) = .1$  KeV,  $r(0) = 6.0$  cm. (b)  $H^+$  ion,  $W_{\perp}(0) = .7$  KeV,  $W_{\parallel}(0) = .3$  KeV,  $r(0) = 6.5$  cm,  $\theta(0) = 90^\circ$ . Ioffe bars are at  $\theta = 0^\circ, 90^\circ, 180^\circ$  and  $270^\circ$ .

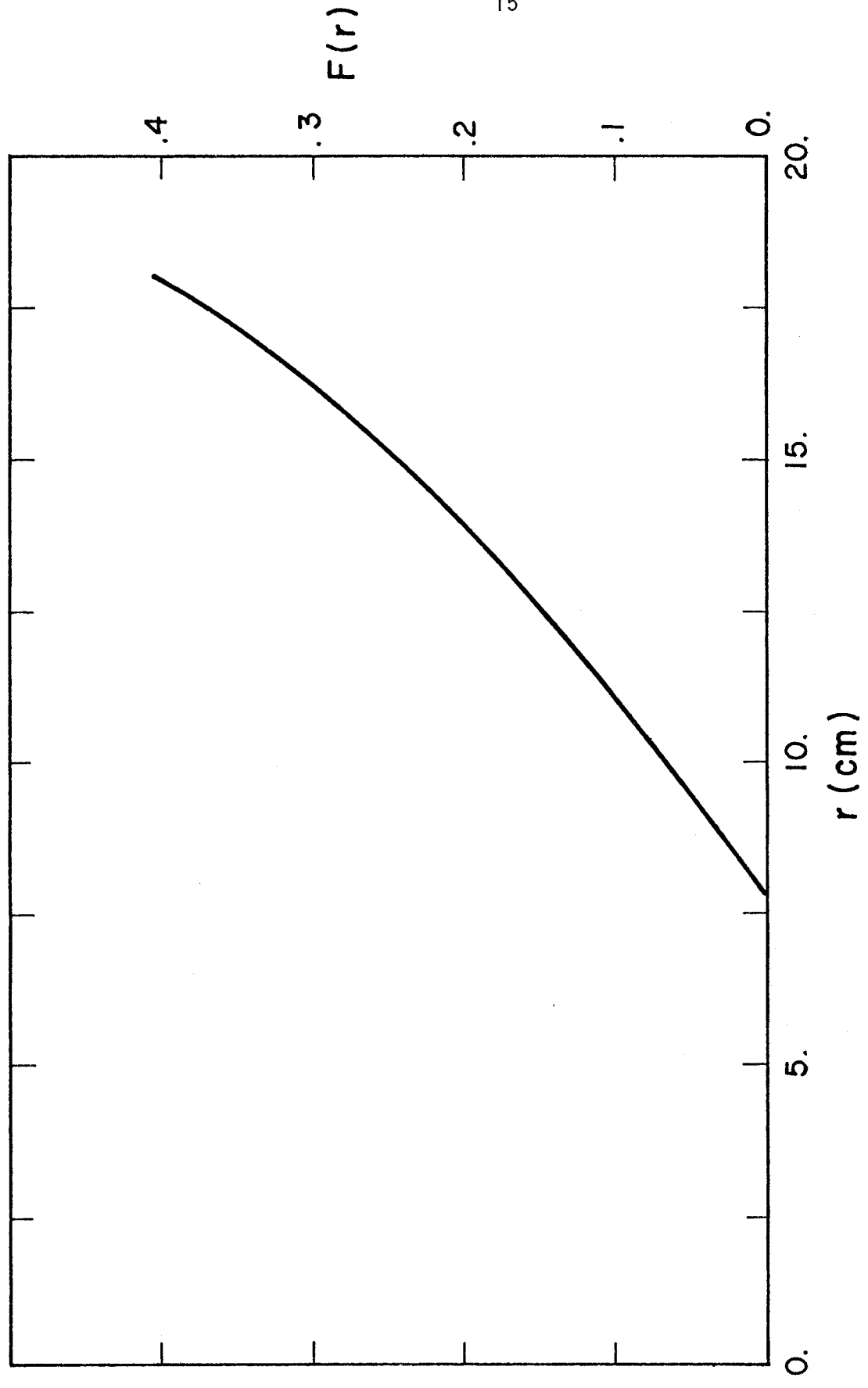


Fig. 6 . Fraction of electrostatically trapped ions lost due to elliptical drift surfaces